Systematic Entomology

Systematic Entomology (2011), **36**, 529–548

Maxfischeriinae: a new braconid subfamily (Hymenoptera) with highly specialized egg morphology

CHARLES ANDREW BORING[1*], BARBARA J. SHARANOWSKI[2*] and MICHAEL J. SHARKEY[1]

[1]Department of Entomology, S-225 Agricultural Science Center North, University of Kentucky, Lexington, KY, U.S.A. and [2]Department of Entomology, 214 Animal Science Bldg., University of Manitoba, Winnipeg, Canada

Abstract. The tribe Maxfischeriini, previously placed in Helconinae, is emended to subfamily status based on morphological and biological evidence. Proposed autapomorphies for Maxfischeriinae include: the presence of a pronotal shelf, forewing vein 1a and 2a present, although 1a nebulous, ventral valve of the ovipositor with serrations from tip to base and specialized egg morphology. The novel, pedunculate egg morphology is described for *Maxfischeria*, representing a new life-history strategy among Braconidae. Based on egg and ovipositor morphology, we suggest that *Maxfischeria* is a proovigenic, koinobiont ectoparasitoid. Five new species of *Maxfischeria* Papp are described with an illustrated key to all species (*Maxfischeria ameliae* **sp.n.**, *Maxfischeria anic* **sp.n.**, *Maxfischeria briggsi* **sp.n.**, *Maxfischeria folkertsorum* **sp.n.** and *Maxfischeria ovumancora* **sp.n.**). In addition to the identification key presented here, all known species of *Maxfischeria* can be separated using the barcoding region of cytochrome *c* oxidase subunit I (*COI*). Based on molecular data, the phylogenetic relationships among the six known species of *Maxfischeria* are as follows: (*M. folkertsorum* **sp.n.** (*M. ovumancora* **sp.n.** (*M. briggsi* **sp.n.** (*M. anic* **sp.n.** (*M. tricolor* + *M. ameliae* **sp.n.**))))).

Introduction

Until now the braconid genus *Maxfischeria* included a single species, *Maxfischeria tricolor* Papp. In the original description, Papp (1994) provisionally proposed the tribe Maxfischeriini within Helconinae for this monotypic genus. Although *M. tricolor* shares similarities with members of Helconinae, Papp (1994) remarked that 'in the future the tribe would [*sic*] be emended to subfamily rank considering its features which differentiate it from all other helconine genera' (p. 143). *Maxfischeria* shares strikingly similar wing venation with members of the tribe Helconini, including relatively complete venation, the presence of forewing vein 1RS, and a complete trapezoidal second submarginal cell in the forewing. However, *Maxfischeria* does not possess other features associated with Helconini, including a distinct lamella on the frons, two strongly developed lateral carinae on metasomal median tergite 1, a long ovipositor relative to the body, a large body size (typically longer than 7 mm), and a complete occipital carina. Thus, the similarities in wing venation, which are plesiomorphic features, are the only characteristics *Maxfischeria* has in common with Helconinae.

Until recently, Papp's hypothesis on the placement of *Maxfischeria* within Helconinae has not been tested. *Maxfischeria* appears to be a non-cyclostome, having a flat labrum and the spiracle of metasomal tergum 2 on the lateral tergite. However, Sharanowski *et al*. (2011) recovered a strongly supported basal clade containing *Maxfischeria*, Aphidiinae and Mesostoinae. This clade was recovered as sister to all remaining cyclostomes. Other multigene analyses have also recovered a basal Mesostoinae + Aphidiinae, providing further evidence for this relationship (Belshaw *et al*., 2000; Zaldivar-Riverón *et al*., 2006). Here we examine morphological and biological

Correspondence: Barbara J. Sharanowski, Department of Entomology, 214 Animal Science Bldg., University of Manitoba, Winnipeg, MB, Canada R3T 2N2. E-mail: Barb.Sharanowski@gmail.com

*These authors made equal contributions to the article.

features of *Maxfischeria* and formally propose Maxfischeriinae as a new subfamily. Additionally, we describe five new species of *Maxfischeria*, and redescribe the holotype of *M. tricolor* Papp to correct previous errors. We also present an identification key for all species, and infer phylogenetic relationships among the species using molecular data.

Biological information about *Maxfischeria* is almost entirely unknown. This lack of information is typical for parasitic Hymenoptera. However, we do find a most unusual egg morphology, which is so striking that it demands further attention. *Maxfischeria* have eggs that are stalked with an umbrella-like anchor, which are unlike any braconid egg yet described. These eggs most closely resemble the specialized eggs of a few Ichneumonidae; however, the eggs of *Maxfischeria* are unique, and any similarity is convergent. Here, we describe this novel egg morphology and make inferences about the biology of *Maxfischeria*.

Material and methods

General morphological terminology follows Sharkey & Wharton (1997). Additionally, malar space was measured as the shortest possible length from the bottom of the eye to the most basal region of the mandible from an anterior view. Tentorial length was taken as the shortest distance between the outer circular margins of the anterior tentorial pits from an anterior view. All specimens of *Maxfischeria* were collected in Australia, stored in 95% ethyl alcohol and dissected in the same solution. Photographs were made with GT ENTOVISION® software using a JVC KY-F75 3CCD digital camera. All mounted specimens were chemically dried using hexamethyldisilazane (HMDS), following the protocol of Heraty & Hawks (1998). For scanning electron microscopy (SEM), specimens were dried with HMDS, coated with gold palladium, and images were taken with a Hitachi S-800 scanning electron microscope. Measurements were taken with a digital micrometer using a Leica MZ12-5 stereoscope. All specimens were compared with the holotype of *M. tricolor*.

Phylogenetic analysis

Initially, 14 specimens, representing all six known species of *Maxfischeria*, were chosen for phylogenetic analysis using the mitochondrial gene cytochrome *c* oxidase subunit I (*COI*). However, of the 14 sequences, eight were discovered to be nuclear-based copies of mitochondrial sequences, or NUMTs (Lopez *et al*., 1994), based on several criteria outlined by Zhang & Hewitt (1996). Thus, the eight NUMT sequences were not used in the analyses, but were submitted to GenBank (accession nos HQ836369–HQ836375). The final phylogenetic analysis included six *Maxfischeria* sequences, representing all six known species (Table 1). An additional three species were incorporated as out-group taxa from three different subfamilies: *Andesipolis* sp. (Mesostoinae) (interpreted as Rhysipolinae; Townsend & Shaw, 2009), *Aphidius rhopalosiphi* (Aphidiinae) and *Doryctes* sp. (Doryctinae). The choice of out-group was based on the phylogenetic position of Maxfischeriinae within the Braconidae, as elucidated in Sharanowski *et al*. (2011). All trees were rooted with *Doryctes* sp.

Sequences were obtained using the protocols outlined below, except for sequences for *Aphidius rhopalosiphi* and *Andesipolis* sp., which were obtained from GenBank (accession nos EU819406 and AY935411, respectively). DNA was extracted from ethanol-preserved specimens following Qiagen protocols in conjunction with the DNeasy™ Tissue Kit (Qiagen, Valencia, CA, U.S.A.). The mitochondrial gene *COI* was amplified using protocols and primers from Schulmeister *et al*. (2002) (*COI* lco hym 5′-CAAATCATAAAGATATTGG-3′ and *COI* hco outout 5′-GTAAATATATGRTGDGCTC-3′). Both product purification and sequencing were performed at the Advanced Genetic Technologies Center, University of Kentucky, using Agencourt CleanSEQ magnetic beads and an Applied Biosystems 3730xl DNA Analyzer, respectively. Contigs were assembled and edited using CONTIG EXPRESS (Vector NTI Advance10™ Invitrogen™). Genbank accession numbers are listed in Table 1. Additional sequenced genes including *28S* and *18S* rDNA, and the protein-coding genes carbamoyl-phosphate synthetase-aspartate transcarbamoylase-dihydroorotase (*CAD*) and acetyl-coenzyme A carboxylase (*ACC*), were uninformative for species-level relationships for *Maxfischeria* (data not shown). We also attempted amplification of the internal transcribed spacer 1 of the rDNA array and the mitochondrial gene cytochrome *c* oxidase subunit II without success.

Alignment was performed using MUSCLE (Edgar, 2004) on the European Bioinformatics Institute (EBI) server. Reading frame accuracy was checked with MEGA 4.0.2 (Tamura *et al*., 2007) using the invertebrate mitochondrial genetic code. Nucleotide frequencies and measures of genetic distance were calculated with MEGA 4.0.2 (Tamura *et al*., 2007). The χ^2 test for homogeneity in base composition was used to test for biases across taxa using PAUP* (Swofford, 2000). To explore the possibility for saturation in the *Maxfischeria* dataset, pairwise Tajima–Nei distances (1984) were plotted against the absolute number of transitions and transversions for each codon position.

Parsimony and Bayesian analyses were performed using TNT 1.0 (Goloboff *et al*., 2003) and MRBAYES 3.1.2 (Huelsenbeck & Ronquist, 2001; Ronquist & Huelsenbeck, 2003), respectively. For both reconstruction methods, the dataset was analysed with all characters included, and with the third position excluded. Additionally, different sets of out-group taxa were analysed to explore the effect of out-group choice on phylogenetic inference. For each parsimony analysis, tree searching was performed with implicit enumeration with 1000 bootstrap replicates. Strict consensus trees were calculated when more than one tree of minimum length was recovered. For the Bayesian analyses, the general time-reversible model with a parameter for invariant sites (GTR + I) was chosen using the program MRMODELTEST 2 (Posada & Crandall, 1998; Nylander, 2004) with PAUP* 4.0b10 (Swofford, 2000), using the PAUPUP graphical interface (Calendini & Martin, 2005).

Table 1. Species of Braconidae analysed in the phylogenetic analysis with corresponding GenBank accession numbers. Voucher numbers are included as a label on all museum-deposited specimens.

Exemplar	Voucher #	Accession #	Locality
Andesipolis sp.	ZISP-Jo753	AY935411[a]	Chile: Flor de Lago
Aphidius rhopalosiphi	Aph-rho-15	EU819406[b]	U.K.: Warwickshire
Doryctes sp.	ZOO12	FJ361239	U.S.A.: West Virginia
Maxfischeria ameliae sp.n.	BJS116	FJ361243	Australia: Queensland
Maxfischeria anic sp.n.	BJS114	FJ361244	Australia: Queensland
Maxfischeria briggsi sp.n.	BJS119	FJ361241	Australia: Queensland
Maxfischeria folkertsorum sp.n.	BJS115	FJ361245	Australia: Queensland
Maxfischeria ovumancora sp.n.	BJS089	FJ361240	Australia: Queensland
Maxfischeria tricolor	BJS088	FJ361242	Australia: Queensland

[a]Zaldivar-Riverón *et al*. (2006).
[b]Traugott *et al*. (2008).

For each analysis, two separate runs with four chains were run for 300 000 generations. Convergence was ascertained using the diagnostics recommended by the authors of the program. Of the 3001 sampled trees, 750 were discarded as burn-in, and a majority rule consensus tree was calculated from the remaining sampled trees.

Results

Phylogenetic analyses

Amplified sequences identified as NUMTs were typically short sequences ranging from 144 to 200 bp. These sequences contained a nearly perfect 51-bp tandem repeat, replicated three or four times across different species of *Maxfischeria*. The tandem repeat was not found in the actual mitochondrial sequences. One of the NUMTs amplified for *Maxfischeria ameliae* **sp.n.** aligned across 470 bp of the mitochondrial *COI* sequences before starting a unique sequence followed by the tandem repeat. All sequences identified as NUMTs were discarded from the dataset.

Alignment of the *COI* sequences resulted in 762 aligned positions, which included 145 parsimony informative sites. Pairwise uncorrected p-distances for all taxa analysed are presented in Table 2. The average distance across all taxa was 0.148 (±0.01 SE), and between out-group and in-group taxa was 0.189 (±0.013 SE). Distances between species of *Maxfischeria* ranged between 0.054 (*M. tricolor* vs *M. ameliae* **sp.n.**) and 0.126 (*Maxfischeria anic* **sp.n.** vs *Maxfischeria folkertsorum* **sp.n.**), with an average of 0.098 (±0.009 SE). These distances are greater than the distances used by other researchers to delimit species using the barcoding region of *COI* for invertebrates (Kartavtsev & Lee, 2006; Smith *et al*., 2007). Table 3 lists the nucleotide frequencies for each codon position and all positions combined. Similar to previous hymenopteran studies (Leys *et al*., 2000; Murphy *et al*., 2008), there is a clear A–T bias in the *COI* dataset, which is extremely pronounced in the third position. Additionally, there is an anti-cytosine bias, which is also exaggerated in the third position. Compositional heterogeneity is only evident in the third position, based on the χ^2 test (Table 3).

Distance measures based on stochastic models can lead to better estimates of multiple substitutions in saturation plots (Sullivan & Joyce, 2005). Thus, the Tajima–Nei distance assuming equal rates of substitution was used to estimate saturation, as the model provides a parameter for base composition. Saturation was inferred when the relationship between genetic distance and the number of transitions or transversions began to disintegrate. These plots, depicted in Fig. 1, demonstrate extreme and moderate saturation in third position transitions and transversions, respectively (Fig. 1c). Even at low genetic distances there is no relationship with the number of transitions at the third codon site. The first position (Fig. 1a) demonstrates some transitional saturation, but there remains a clear relationship through most of the data points. Second-position (Fig. 1b) transitions and transversions are not saturated. However, the severe saturation of transitions in the third position has a large effect on the overall dataset (Fig. 1d). Thus, it is highly probable that the third position will contribute more noise than phylogenetic signal.

In the maximum parsimony analysis one most parsimonious tree, of length (L) 433 steps, was recovered when all data were included in the analysis (consistency index, CI = 0.704; retention index, RI = 0.486) (Fig. 2a). One minimum length tree was also recovered when the third position was excluded from the parsimony analysis (L = 131; CI = 0.824, RI = 0.733) (Fig. 2b). These trees were very similar, although the analysis with all data included recovered (*M. ameliae* **sp.n.** (*M. anic* **sp.n.** + *M. tricolor*) (Fig. 2a) versus (*M. anic* **sp.n.** (*M. ameliae* **sp.n.** + *M. tricolor*) when the third position was excluded (Fig. 2b). The cladogram generated from the dataset lacking the third position had higher bootstrap support for most clades. Regardless of out-group selection, relationships among species of *Maxfischeria* remained stable when the third position was excluded (data not shown).

Bayesian analyses were very similar, although there was less resolution when all data were included, particularly between *Maxfischeria ovumancora* **sp.n.** and *Maxfischeria briggsi* **sp.n.** (Fig. 2c, d). Posterior probabilities were also reduced for some clades when all data were included. In-group relationships were identical between the parsimony and Bayesian trees when the third position was excluded

Table 2. Uncorrected p-distances for each species examined.

	1	2	3	4	5	6	7	8
1. *Doryctes* sp.								
2. *Aphidius rhopalosiphi*	0.163							
3. *Andesipolis* sp.	0.159	0.141						
4. *Maxfischeria ameliae* **sp.n.**	0.196	0.163	0.167					
5. *Maxfischeria anic* **sp.n.**	0.209	0.191	0.196	0.076				
6. *Maxfischeria briggsi* **sp.n.**	0.213	0.176	0.176	0.098	0.109			
7. *Maxfischeria folkertsorum* **sp.n.**	0.202	0.189	0.198	0.096	0.126	0.120		
8. *Maxfischeria ovumancora* **sp.n.**	0.217	0.165	0.174	0.072	0.100	0.102	0.098	
9. *Maxfischeria tricolor*	0.191	0.187	0.185	0.054	0.096	0.120	0.111	0.098

Table 3. Nucleotide frequencies for each codon position for cytochrome *c* oxidase subunit I (*COI*) sequences and χ^2 test for base composition bias across species for each codon position and associated significance value (P) ($df = 24$).

	First position				Second position				Third position				All positions			
Taxon	T	C	A	G	T	C	A	G	T	C	A	G	T	C	A	G
Doryctes sp.	33.5	9.8	33.1	23.6	48.8	18.5	15.4	17.3	52.6	0.8	38.7	7.9	44.9	9.7	29.0	16.3
A. rhopalosiphi	31.1	9.3	37.2	22.4	47.8	21.4	14.3	16.5	54.9	0.5	41.8	2.7	44.6	10.4	31.1	13.9
Andesipolis sp.	29.4	10.0	33.3	27.4	47.3	21.9	13.9	16.9	50.2	0.5	41.8	7.5	42.3	10.8	29.7	17.2
M. ameliae **sp.n.**	33.1	9.4	34.3	23.2	48.0	16.9	16.5	18.5	53.0	0.0	42.7	4.3	44.7	8.8	31.1	15.4
M. anic **sp.n.**	33.6	9.7	34.4	22.3	48.8	16.8	16.0	18.4	51.4	0.0	36.0	12.6	44.6	8.8	28.9	17.8
M. briggsi **sp.n.**	34.8	10.1	33.3	21.7	49.5	18.2	15.7	16.7	52.0	1.5	36.7	9.7	45.4	10.0	28.5	16.0
M. folkertsorum **sp.n.**	32.3	9.4	34.3	24.0	48.0	17.3	17.3	17.3	51.8	1.2	41.9	5.1	44.0	9.3	31.1	15.5
M. ovumancora	33.5	9.1	35.0	22.4	48.4	16.9	17.3	17.3	54.2	0.4	39.5	5.9	45.3	8.8	30.6	15.2
M. tricolor	33.3	9.1	35.0	22.6	48.1	16.5	17.3	18.1	52.7	0.8	35.8	10.7	44.7	8.8	29.4	17.1
Average	32.8	9.5	34.4	23.3	48.3	18.1	16.1	17.5	52.5	0.6	39.4	7.4	44.5	9.4	30.0	16.1
χ^2	4.29				6.45				37.27				11.48			
P	0.99				0.99				0.04				0.98			

(Fig. 2b, d). The Bayesian analysis generated from the dataset excluding the third positions converged on the same tree as that of the parsimony analysis for in-group relationships (Fig. 2c), but did not recover *Aphidis rhopalosiphi* + *Andesipolis* sp. as sister to all species of *Maxfischeria*.

Egg morphology

Two female specimens of *M. ovumancora* **sp.n.** were dissected to examine the morphology of the eggs. The dissections revealed several mature eggs, all in the same stage of development (Fig. 3a). Each egg had an elongate–oval shape with a well-sclerotized chorion (Fig. 3b). On one end of each egg was a highly sclerotized stalk, ending in an 'anchor' (Figs 3a, 3b). One of the dissected specimens displayed the position of an egg ready to be laid, with the anchor inserted into the base of the ovipositor (Figs 3c–f).

Discussion

Phylogenetics of Maxfischeria

Although there is significant genetic variation among species of *Maxfischeria* in *COI* (5–13% genetic distance), there is little morphological variation across species. However, all species can be delineated based upon the barcoding region of *COI*, in addition to the morphological identification key presented below, which is primarily based upon colour. As a result of the amplification of NUMTs, we were only able to obtain genetic data for one specimen per species, and thus were unable to determine intraspecific genetic variation. Therefore, it is possible that future evidence may indicate a greater number of species than the morphospecies delineated herein.

Clearly the third position added ambiguity to the dataset, indicated by lower resolution, a lower retention index, sensitivity to out-group selection, and lower nodal support for recovered clades when compared with the analyses that excluded the third position. Analyses with the third position excluded were robust to both method of analysis and out-group selection. Thus, the relationships shown in Fig. 2b, d are preferred. Given the evidence, the most probable relationships among all known species of *Maxfischeria* are as follows: (*M. folkertsorum* **sp.n.** (*M. ovumancora* **sp.n.** (*M. briggsi* **sp.n.** (*M. anic* **sp.n.** (*M. tricolor* + *M. ameliae* **sp.n.**))))) (Fig. 2d). However, there is some ambiguity in the relationships among (*M. anic* **sp.n.** (*M. tricolor* + *M. ameliae* **sp.n.**)), as these clades were not recovered in more than 50% of the 1000 bootstrap replicates in the parsimony analysis.

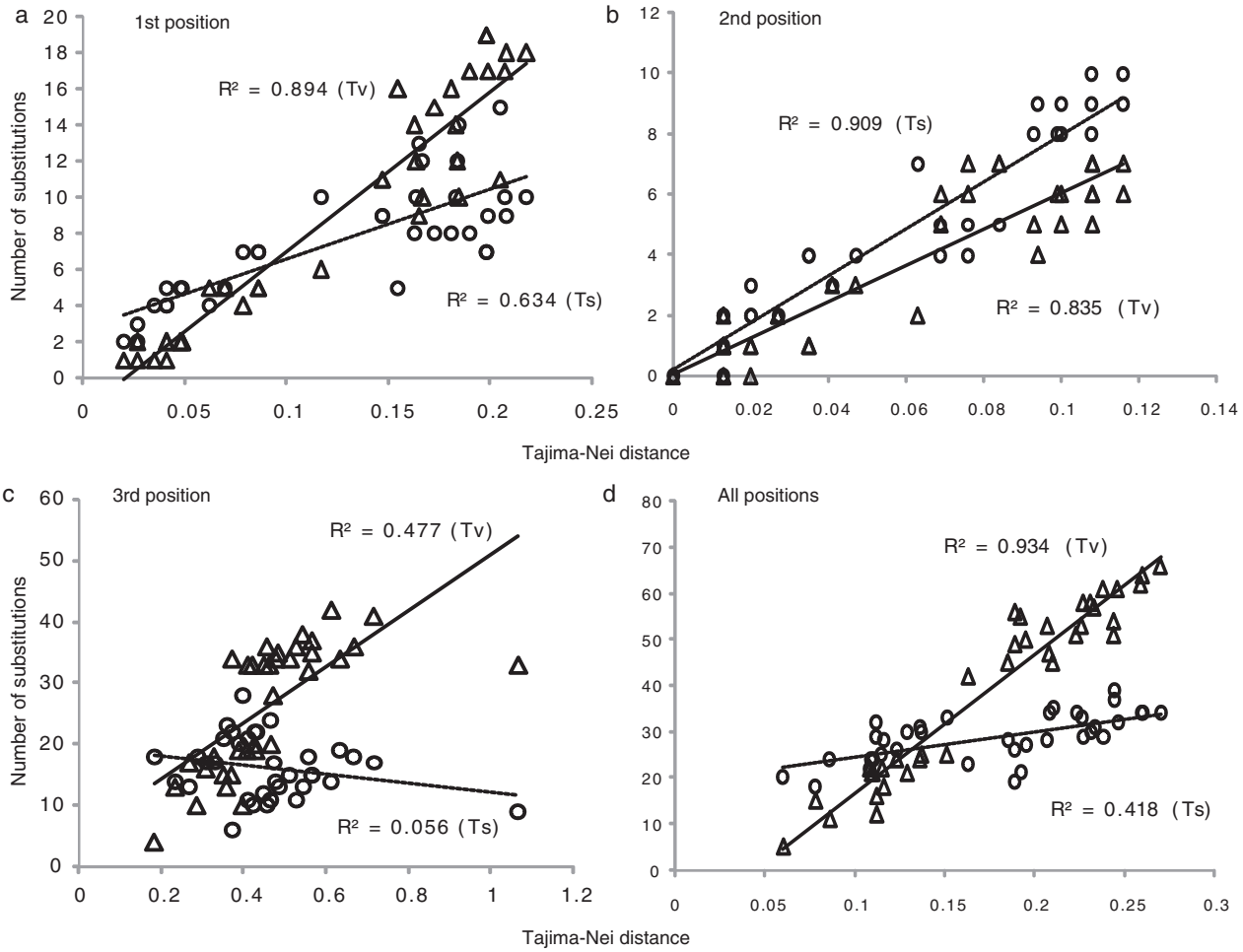

Fig. 1. (a–d) Tajima–Nei distance plots against the absolute number of transitions (Ts; ◯) and transversions (Tv; △) for each codon position and all data combined.

Morphological evidence for subfamily status

The monophyly of Maxfischeriinae is supported by morphological evidence: the specialized egg morphology; the presence of a pronotal shelf; forewing veins 1a and 2a being present, although 1a is nebulous; and ventral valve of the ovipositor with serrations from tip to base are putative autapomorphies for this subfamily. Because of the rarity of additional specimens for dissection, only two species have been confirmed with specialized eggs (see egg morphology below). Further sampling is necessary to determine the taxonomic range of this feature. The monophyly of Maxfischeriinae was also supported with molecular evidence by Sharanowski *et al*. (2011).

In the following, we examine Papp's (1994) treatment of *Maxfischeria* to clarify the distinction between Maxfischeriinae and Helconinae. Papp (1994) treated Maxfischeriini as a tribe of Helconinae, and remarked 'that in the future the tribe would be emended to subfamily rank, considering the features that differentiate it from all other helconine genera: (i) head entirely smooth (i.e. frons without midlongitudinally raised carina, occipital and hypostomal carina absent); (ii) pronope absent; (iii) hind femur entirely smooth; (iv) hind trochanter rather slender; (v) forewing, vein 1-SR present (=1RS), m–cu antefurcal (=1m–cu), veins 2A and a present (=1a and 2a, respectively) and cross-vein r–m present; (vi) hindwing, cu–a subvertical; (vii) pair of spiracles somewhat anteriorly from middle of propodeum; (viii) maxillary palp with six segments and labial palp with four segments; (ix) prescutellar sulcus and lateral field of scutellum (or axilla) smooth (i.e. not crenulate) (pp. 143–144). It must have been the combination of these characters that distinguished *Maxfischeria*, because the diagnostic wing venation can also be found among Helconini genera. *Maxfischeria* does not possess other features associated with Helconini, including a distinct lamella on the frons, two strongly developed lateral carinae on metasomal median tergite 1, a long ovipositor relative to the body, a large body size (typically longer than 7 mm) and a complete occipital carina. Thus, similar wing venation is a plesiomorphic feature, and it is understandable

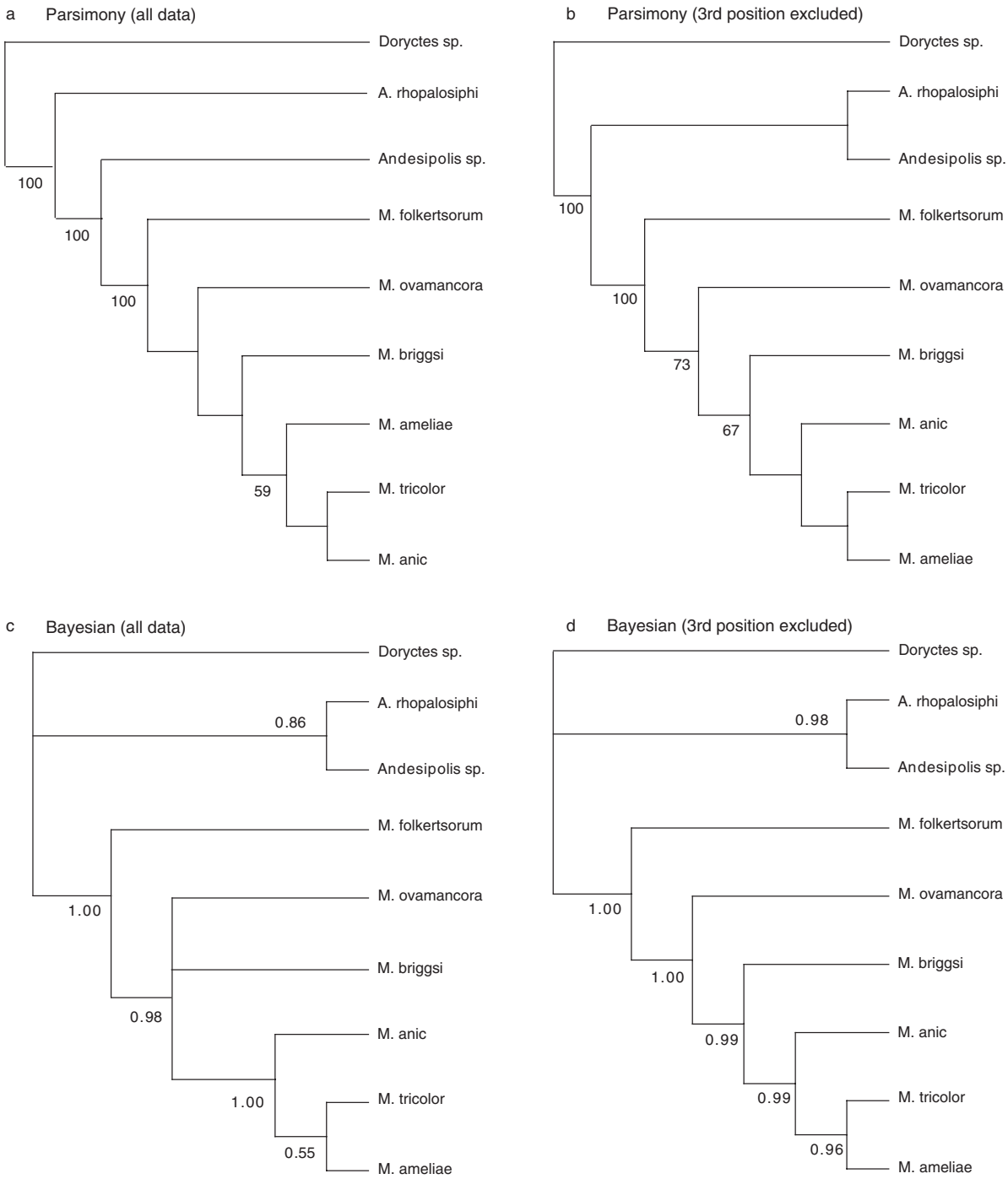

Fig. 2. (a) Shortest length tree (L = 433 steps) recovered from parsimony analysis with all data included. (b) Shortest length tree (L = 131 steps) recovered from parsimony analysis with third position excluded. (a, b) Numbers below the node indicate bootstrap values. (c) Majority rule tree from Bayesian analysis with all data included. (d) Majority rule tree from Bayesian analysis with third position excluded. (c–d) Numbers below the node indicate posterior probabilities.

that *Maxfischeria* was provisionally placed within Helconinae. Furthermore, all Helconini genera have a smooth hind femur, except *Wroughtonia* Cameron and some species of *Helcon* Nees. Several genera of Helconinae possess the same palpal formula, especially those within the Helconini. The propodeal spiracles are situated in the same location as those of members of Helconinae. Finally, although reduced, the hypostomal carina is present in species of *Maxfischeria* (Fig. 4b,

see arrow). The diagnoses and descriptions of Maxfischerinae and *Maxfischeria* (see below) contain a more accurate set of morphological features to distinguish species of *Maxfischeria* from members of the Helconinae and other braconids in general.

Egg morphology

The stalked eggs illustrated for *M. ovumancora* **sp.n.** (Figs 3a, b) have never been described for any other member of Braconidae. Pedunculate eggs with an anchor are found in a select group of Ichneumonidae, including the Anomaloninae, Lycorininae, Stilbopinae and Tryphoninae. All ichneumonids with pedunculate eggs and a known biology are koinobiont. It is possible that Maxfischeriinae are also koinobiont. Some comparisons between *Maxfischeria* egg morphology and that of select species of Ichneumonidae are made below.

The Anomaloninae are koinobiont endoparasitoids that attack larval Lepidoptera or Coleoptera, and emerge from the host pupae (Wahl, 1993). Anomalonine eggs have been illustrated by both Gauld (1976) and Iwata (1960). Both illustrations show an egg with a short, robust stalk ending in an anchor. Gauld (1976) suggested that the anchor in *Heteropelma* spp. is used to secure the egg to tissue within the host.

The egg shape and colour of *Maxfischeria* is similar to that of one particular species of Stilbopinae, *Panteles schnetzeanus* (Roman): the latter has a strongly recurved 'tail' on its egg, but lacks an anchor (Quicke, 2005). Quicke (2005) demonstrated that these eggs are laid completely within the host, and that the recurved 'tail' is embedded in host tissue, most commonly in Malpighian tubules, the rectum or other tissue in the posterior region of the host.

Lycorininae eggs also share similarities to the eggs of *Maxfischeria*, particularly the shape of the egg and anchor, and location of the stalk and anchor. However, there are striking differences: the ovarian eggs of Lycorininae are synovigenic, have membranous tissue surrounding the egg that modifies the position of the anchor and mature eggs are described as being white (Coronado-Rivera *et al*., 2004; Shaw, 2004), whereas the ovarian eggs of *Maxfischeria* are probably proovigenic (see below), have a membranous tissue around the egg that does not modify the position of the anchor and the eggs have a tint of sclerotized colour (Figs 3a, b). The Lycorininae have an enigmatic biology, with only a few host association records. Observations by Coronado-Rivera *et al*. (2004) and Shaw (2004) showed that this group contains koinobiont parasitoids that complete their development as an ectoparasitoid. There still remains uncertainty concerning the biology of early instar Lycorininae larvae: they may be ectoparasitic (presumably in the hindgut) or endoparasitic (Coronado-Rivera *et al*., 2004).

Members of the ichneumonid subfamily Tryphoninae are ectoparasitic, and attach the egg to the host in a variety of ways (Kasparyan, 1981). Some tryphonines have an unmodified egg that is shallowly embedded within the host so that part of the egg still protrudes from the exterior surface of the host (Clausen, 1932; although see Mason, 1967; Kasparyan, 1981). In other Tryphoninae, the egg has a modified structure to attach to the host. Clausen (1932) described these eggs as having a shield-shaped structure that opens, umbrella-like, when laid. Clausen (1932) illustrated the egg of *Tryphon bidentatus* Stephens (as *Tryphon incestus* Holmgren), and how the anchor is embedded in the groove between the head and the first thoracic segment of the host larva. The illustration shows that *Maxfischeria* and *T. bidentatus* have similarly shaped eggs; a notable difference is that the eggs of *Maxfischeria* have a flange on the anchor (Fig. 3b). To our knowledge, this flange is unique to *Maxfischeria*. The eggs of *T. bidentatus* were described as having an exceedingly tough, yellowish chorion, which is a fitting description for the eggs of *Maxfischeria* (Fig. 3b). The similarity in egg morphology between *Maxfischeria* and *Tryphon* spp. is obviously the result of convergence.

Interestingly, the egg of *Maxfischeria* is nearly as long as the ovipositor (Figs 3c–e), and only the base of the ovipositor is as wide as the egg. This raises questions about the means by which the egg passes through the ovipositor. It is apparent that the flange at the apex of the anchor (Fig. 3b, see arrow) is first to enter the ovipositor (Figs 3e, f). Further examination of this dissection under SEM revealed how the dorsal valve accommodates this flange: the ventral surface of the dorsal valve that forms the egg canal has a groove along its length (Figs 3e, 5b). The inside of this grove could not be observed. The groove is incomplete; the dorsal surface of the dorsal valve is undivided. The dimensions of the egg canal appear to approximately match those of the anchor (Fig. 3f), making it difficult to imagine the entire egg passing through this space. Given the relative size of the egg to that of the ovipositor, there is reason to suspect that only the anchor passes through the egg canal, with the stalk travelling between the ventral valves, and the remainder of the egg travelling exterior to the ovipositor. If this is the case, then it would suggest that this type of egg passage is highly similar to some members of Tryphoninae (Ichneumonidae) with modified eggs. From the similarities *Maxfischeria* share with Tryphoninae, we suggest that species of *Maxfischeria* are koinobiont ectoparasitoids.

It is possible that *Maxfischeria* is pro-ovigenic. The strongest evidence to support this biology is from direct observation of the metasomal (i.e. abdominal) body cavity through dissection. Dissections of *M. ovumancora* **sp.n.** revealed several mature eggs that were all in the same stage of development (Fig. 3a), and no undeveloped eggs were identified. We were also able to see through the metasoma of one specimen of *M. tricolor*, and the outline of a similar egg morphology can clearly be seen. This indicates that the egg shape is not unique to *M. ovumancora* **sp.n.**, but it has yet to be determined if all other species have exactly the same egg morphology. Jervis *et al*. (2001) describes egg maturation strategies as a continuum of ovigeny, where strict pro-ovigeny is rare. Ellers & Jervis (2004) identified parameter ranges that are most likely to lead to strict pro-ovigeny, and all scenarios

with very large egg size led to strict pro-ovigeny. The eggs of *M. ovumancora* **sp.n.** are large, approximately 0.7 mm in length (Fig. 3b), supporting the probability of pro-ovigeny, despite the rare frequency of this biology. Independent re-evaluation with additional specimens is encouraged. As the two specimens of *M. ovumancora* **sp.n.** that were dissected were also collected together, it remains possible that they are synovigenic, with their final compliment of eggs developed at the time of collection.

Taxonomy

Subfamily Maxfischeriinae Papp subfam.n.

Type species. Maxfischeria tricolor Boring & Sharanowski, 1994.

Diagnosis. This subfamily can be distinguished from other Braconidae by the following combination of characters: presence of pronotal shelf (Fig. 4d); notauli absent medially, present only anterolaterally; mesonotal mid-pit present (Fig. 4e); tarsal claws with a well-developed basal lobe; apex of scutellum smooth and shiny, posterior scutellar depression absent (Fig. 4f, see arrow); scutellar sulcus smooth; forewing veins 1a and 2a present, although 1a nebulous (Fig. 5c); six maxillary palpomeres, with the fourth palpomere as long or longer than the sixth; forewing vein 1RS long; sternaulus appearing as an ovoid depression at mid-length of mesopleuron (Fig. 4c); ovipositor short, dorsal valve smooth and enlarged near apex, ventral valve with serrations along entire length (Fig. 5a).

Description. Head smooth, vertex covered with setae; occipital carina absent; hypostomal carina present; interantennal carina absent; eye without setae; six maxillary palpomeres; four labial palpomeres; pronotum with an anterior projection, narrowing anteriorly to blunt knob; mesosoma with epicnemial carina present; mid-pit present; scutellar sulcus smooth; forewing 1RS present, m–cu antefurcal, 2a present, 1a nebulous, (RS + M)b present, 1cu–a subvertical; hindwing 2RS and 3M tubular, with 3M nearly reaching wing margin; dorsope absent; propodeal spiracle situated somewhat anteriorly (Fig. 4f); ovipositor short, dorsal valve smooth and enlarged near apex, ventral valve with serrations along entire length (Fig. 5a), ovipositor sheath with ventrally directed setae concentrated on the ventral margin.

Remarks. Putative autapomorphies for Maxfischeriinae include: presence of a pronotal shelf or projection (Fig. 4d), forewing vein 1a and 2a present, although 1a nebulous; ventral valve of the ovipositor with serrations from tip to (exposed) base; and pedunculate eggs (Fig. 3b). This subfamily currently contains a single genus, *Maxfischeria*. Species of *Maxfischeria* key out to Helconinae in couplet 66 in van Achterberg (1993) and can be separated from members of Helconinae with the absence of an occipital carinae and presence of a pronotal shelf. Members of Maxfischeriinae run to couplet 23 in Sharkey's (1993) key to braconid subfamilies. This couplet is modified to accommodate Maxfischeriinae as follows.

23(21) a. Head without occipital carina. . .23A
aa. Head with occipital carina. . .25

23A(23) a. Pronotal shelf present
b. Mid-pit present . . .Maxfischeriinae
aa. Pronotal shelf absent
bb. Mid-pit absent . . .24

Genus *Maxfischeria* Papp, 1994

Type species. Maxfischeria tricolor Papp, 1994. This monotypic genus was described by Papp (1994). This description fits the genus well, except that the hypostomal carina is present in *Maxfischeria* (Fig. 4b, see arrow). Additionally, the forewing is clear basally and infuscate apically.

Diagnosis. Currently, *Maxfischeria* is the only known genus within Maxfischeriinae. Thus, the diagnosis for the subfamily suffices for the genus.

Distribution. All known species are found in Australia. Specimens have been collected from the following states: Australian Capital Territory, New South Wales, Queensland and Tasmania.

Remarks. The majority of specimens examined in this study have been collected at night with a mercury vapour or ultraviolet light. This may indicate that species of *Maxfischeria* are nocturnal; however, their bright coloration suggests that they may also be active during the day.

Key to known species of *Maxfischeria*

1. Length of malar space approximately one-half the length between the tentorial pits from anterior view, ratio malar space: tentorial length 0.52–0.67 (Fig. 6a) 2
– Length of malar space much less than one-half the length between the tentorial pits (1/6–1/3) from anterior view, ratio malar space: tentorial length 0.18–0.36 (Fig. 4a) 3

2. Forewing vein 1RS less than half the length of forewing vein r, ratio 1RS/r approximately 0.33–0.47; forewing vein r approximately three-quarters the length of forewing vein 3RSa, ratio r/3RSa 0.76–0.78; metasomal median tergite 1 entirely black (Fig. 7f) . . . . . *Maxfischeria folkertsorum* **sp.n.**
– Forewing vein 1RS more than half the length of forewing vein r, ratio 1RS/r approximately 0.51–0.67; forewing vein r subequal to forewing vein 3RSa, ratio r/3RSa 0.88–0.93; metasomal median tergite 1 white with black spot (Fig. 7d) 5

3. Hindwing vein 2–1A distinctly present and tubular (Fig. 5c) 4
– Hindwing vein 2–1A absent or occasionally present as an extremely small nub-like projection from 1–1A..... *Maxfischeria tricolor*

4. Propodeum with dull, shallow anterior longitudinal median carina (Fig. 4f); metasomal tergites 1–2 entirely black; metasoma lateral tergite 3 with a black sclerotized band (Figs 6b, e); hypopygium desclerotized medially from ventral view (Fig. 6f); head and propodeum melanic to dark brown (Fig. 6d) ..... *Maxfischeria ovumancora* **sp.n.**
– Propodeum with very sharp anterior longitudinal median carina; metasomal tergites 1–2 mostly white (occasionally with some brown or black pigmentation medially) (Fig. 7e); metasoma lateral tergite 3 typically without a black sclerotized band (very rarely with a small black spot) (Fig. 8a); hypopygium entirely sclerotized; head yellow; propodeum orange-brown (Fig. 8a) ..... *Maxfischeria ameliae* **sp.n.**

5. Hindwing vein 2–1A present but short; propodeum sculptured, with at least an anterior median carina, areola and other irregular sculpturing; hypopygium without pigmentation (Fig. 9d); metasomal tergite 2 mostly white (Fig. 7b)..... *Maxfischeria briggsi* **sp.n.**
– Hindwing vein 2–1A absent; propodeum almost devoid of sculpture medially, possibly with very dull anterior median carina, but otherwise smooth; hypopygium pigmented laterally (Fig. 9a), metasomal tergite 2 entirely black (Fig. 7d) ..... *Maxfischeria anic* **sp.n.**

Maxfischeria ameliae Boring & Sharanowski sp.n.
(Figs 7e; 8a–d)

Diagnosis. This species can be distinguished from all other species of *Maxfischeria* by the following combination of characters: head yellow; length of malar space much less than one-half the length between the tentorial pits; propodeum orange-brown (Fig. 8a); propodeum with very sharp anterior longitudinal median carina; hindwing vein 2–1A distinctly present and tubular; metasomal tergites 1–2 mostly white (occasionally with some brown or black pigmentation medially) (Fig. 7e); metasoma lateral tergite 3 typically without a black sclerotized band (very rarely with a small black spot) (Fig. 8a); hypopygium entirely sclerotized.

Material examined. Holotype, 1♀, Australia, Queensland, Carnarvon Gorge National Park ranger station at light, 25°0′41″S, 148°02′03″E, 25 November 2005. N. Schiff. Deposited at Australian National Insect Collection (ANIC), The Commonwealth Scientific and Industrial Research Organisation (CSIRO), Canberra, ACT, Australia.

Paratypes, 3♀, Australia: (2♀) Queensland Carnarvon Gorge National Park ranger station at light, 25°0′41″S, 148°02′03″E, 25 November 2005. N. Schiff. Deposited at ANIC, CSIRO, Canberra, ACT, Australia; (1♀) upper Jardine River, Cape York Pen, N. Qld 11°10′S, 142°37′E, 27 October 79. M.S. and B.J. Moulds. Deposited at the Australian Museum, Sydney, Australia.

Description. Length: 5.9–6.5 mm. Colour: head yellow with black confined within ocellar triangle (Fig. 8b); maxillary and labial palpi yellow; antenna brown; base of mandible yellow with light brown near the apex; pronotum, propleuron and mesoscutum blackish brown, scutellum and metanotum light brown, mesopleuron irregularly blackish brown to light brown laterally, and blackish brown ventrally (Fig. 8a), propodeum light brown; foreleg yellow, except for brown trochantellus, mid-leg coxa and trochantellus blackish brown, femur light brown fading to yellow apically, tibia and tarsomeres yellow, hindleg blackish brown; tegula light brown; wings basally hyaline, apically infuscate, and with a medial hyaline streak (Fig. 8a); metasomal median tergite 1 with light-brown circular coloration (Figs 7e, 8c), median tergite 2 white, median tergites 3–7 white, with black bands on anterior margin, median tergite 8 entirely black; metasomal sterna white except sternites 4–6 white with black bands on anterior lateral margins that do not meet ventrally (Fig. 8c); ovipositor sheath testaceous basally and light brown apically, ovipositor testaceous. Head: antenna with 45–50 flagellomeres, terminal flagellomere with apical spine; ratio of malar space/tentorial length 0.34–0.36. Mesosoma: propodeum with sharp anterior longitudinal median carina dividing large anterior median depression, elliptical-shaped depression present just below median carina, medial to posteromedial region smooth, posterolateral depression bordered by carinae along posterior and lateral margin, setae concentrated laterally. Wings: vestigial hindwing costal vein present, vein 2–1A present, although vestigial; number of hamuli variable, with four hamuli on left wing and five hamuli on right wing. Metasoma: hypopygium sclerotized medially.

Distribution. This species is known from the type locality in central Queensland and from Cape York Peninsula in northern Queensland, Australia.

Remarks. Variation in the three paratypes is as follows. Paratype 1: foreleg entirely yellow, coxa and trochanter of mid leg brown, mid-leg femur, tibia and tarsus yellow; coxa, trochantellus, and femur of hindleg light brown, tibia and tarsus black; metasomal tergum 3 with light-brown spot instead of solid black bar; four hamuli. Paratype 2: apical flagellomere pointed, but not with a distinct spine; foreleg entirely yellow; coxa and trochanter of mid leg brown; metasomal tergum 3 with black spot instead of solid black bar; hindwing vein 2–1A present but short; five hamuli on left wing, four hamuli on right wing. Paratype 3: mesosoma with slightly more orange than black coloration. Male: unknown.

Etymology. The specific epithet is a genitive noun, named in honour of B. Sharanowski's niece, Amelia Grace Brant, born to Julie and Billy Brant on 9 December 2008 in Townesville, Queensland, Australia.

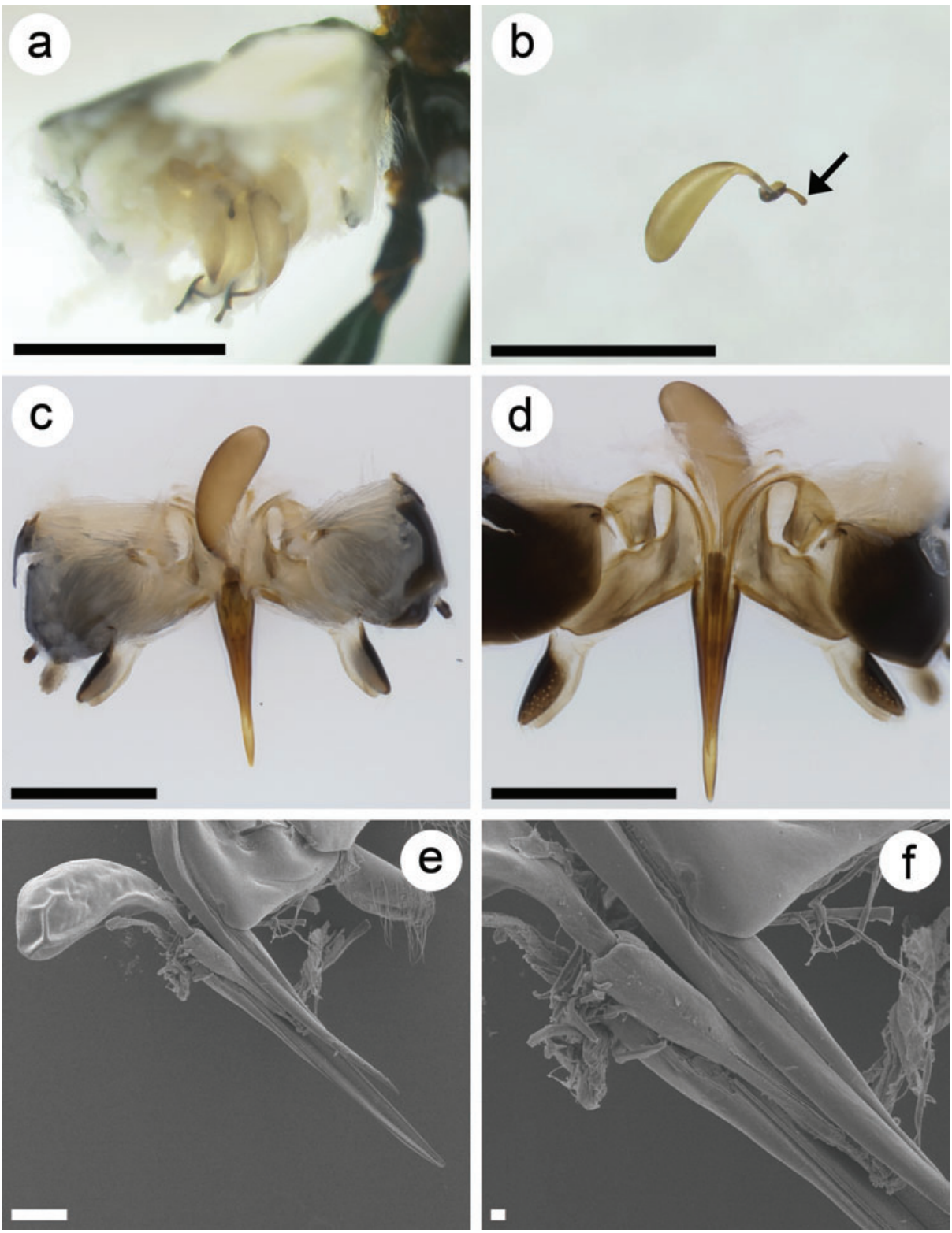

Figs 3a–f. *Maxfischeria ovumancora* **sp.n.**: a, lateral metasoma partially dissected, scale bar 1 mm; b, egg, scale bar 0.9 mm; c, dorsal view of dorsal valve and dissected posterior metasoma, scale bar 0.5 mm; d, ventral view of ventral valves and dissected posterior metasoma, scale bar 0.5 mm; e, ventral view ovipositor with one ventral valve removed and the apical portion of the egg within the egg canal, scale bar 100 μm; f, higher magnification of Fig. 3e, where the apical portion of the egg is within the egg canal, scale bar 10 μm.

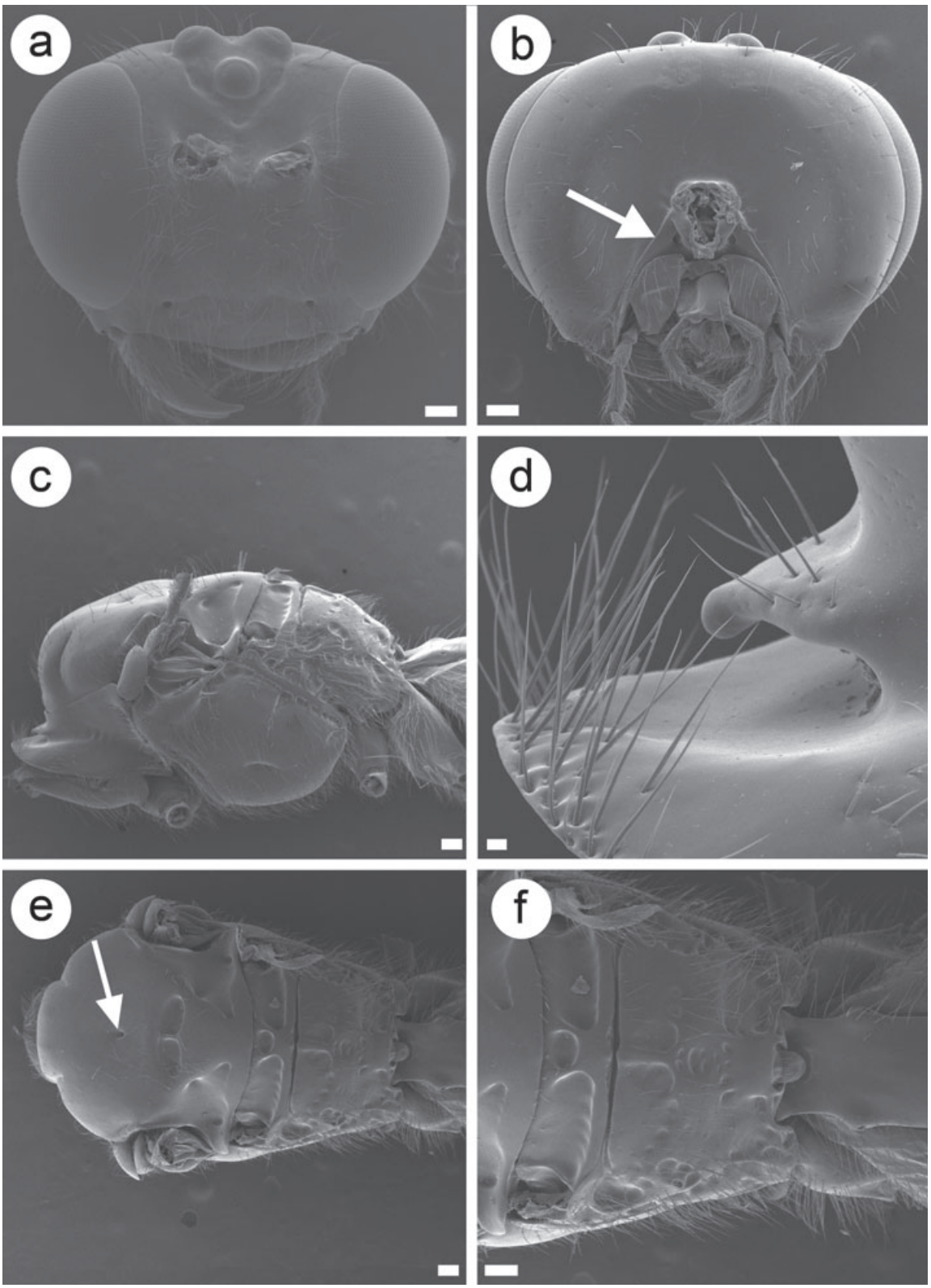

Figs 4a–f. *Maxfischeria ovumancora* **sp.n.**: a, anterior head, scale bar 100 μm; b, posterior head, scale bar 100 μm, arrow points to hypostomal carina; c, lateral metasoma, scale bar 100 μm; d, pronotal shelf, scale bar 10 μm; e, dorsal metasoma, arrow points to pit on median mesonotal lobe, scale bar 100 μm; f, propodeum, scale bar 100 μm, arrow points to absence of posterior scutellar depression.

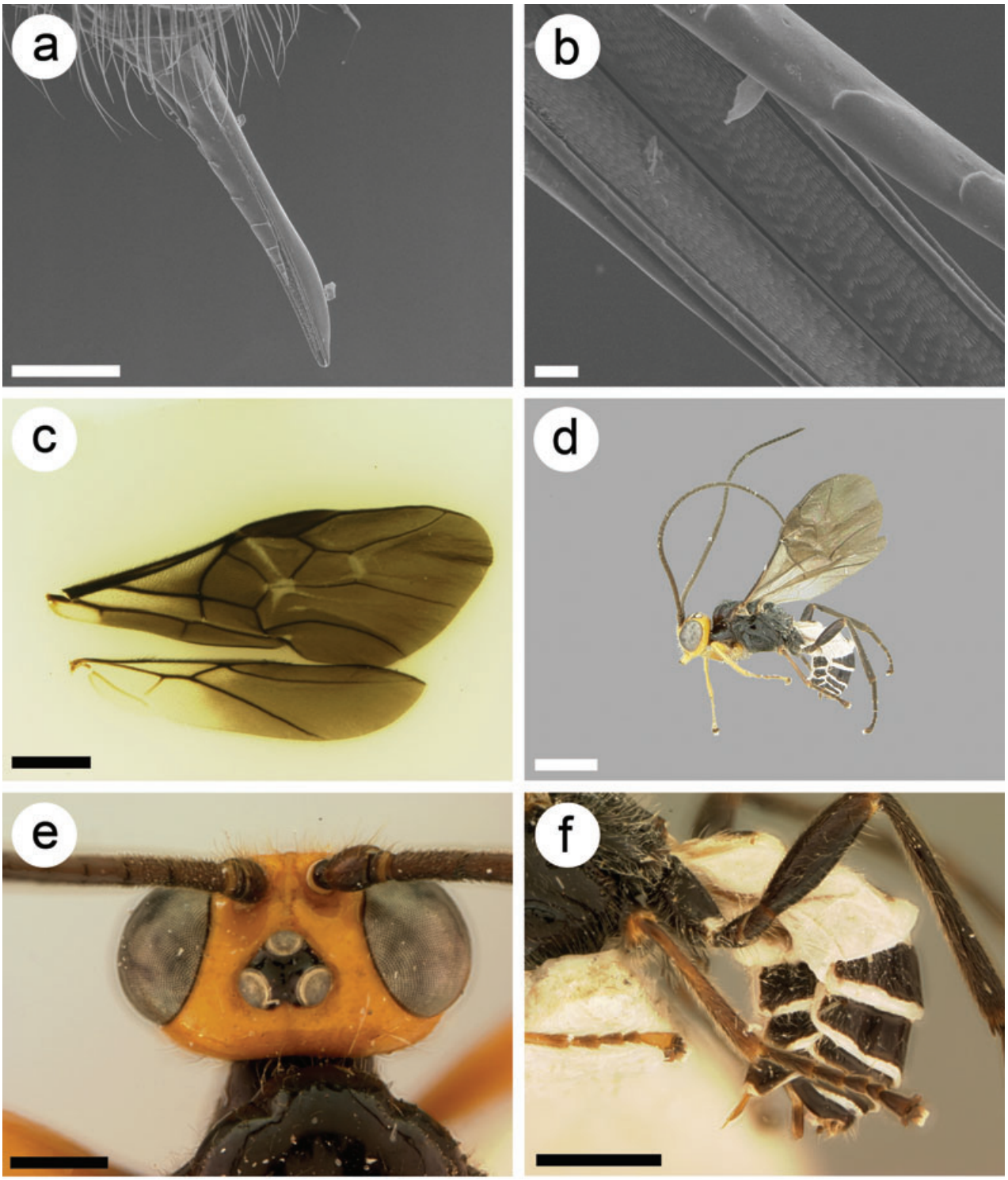

Figs 5a–f. a–c, *Maxfischeria ovumancora* **sp.n.**: a, lateral ovipositor, scale bar 50 μm; b, ventral view of dorsal ovipositor valve, scale bar 10 μm; c, forewing and hindwing, scale bar 1 mm; d–f, *Maxfischeria tricolor* (holotype): d, lateral habitus, scale bar 2 mm; e, dorsal head, scale bar 0.5 mm; f, lateral metasoma, scale bar 1 mm.

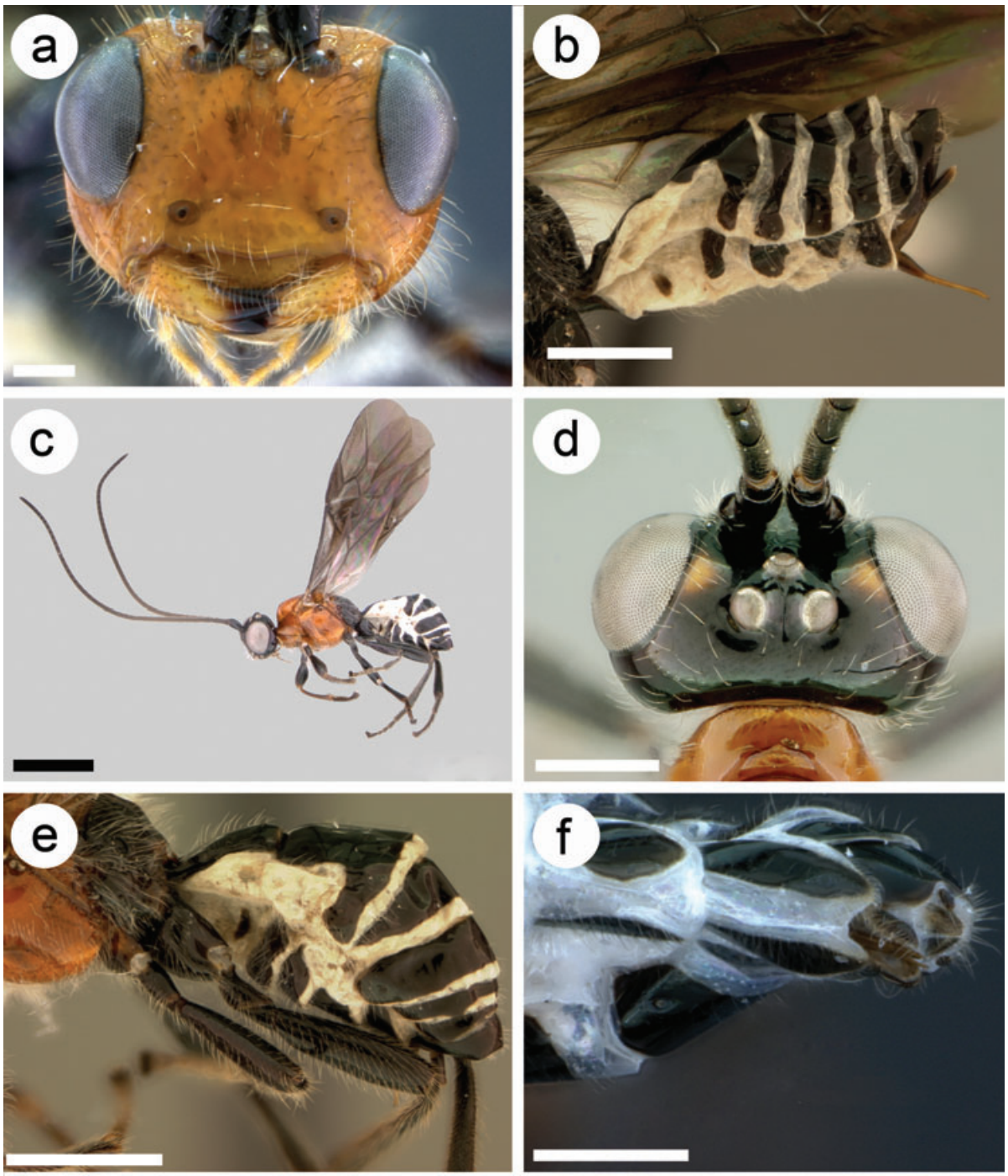

Figs 6a–f. a–b, *Maxfischeria folkertsorum* **sp.n.**: a, anterior face, scale bar, 0.25 mm; b, lateral metasoma, scale bar 1 mm. c–f, *Maxfischeria ovumancora* **sp.n.**: c, lateral habitus, scale bar 2 mm; d, dorsal head, scale bar 0.5 mm; e, lateral metasoma, scale bar 1 mm; f, ventral metasoma, scale bar 0.5 mm.

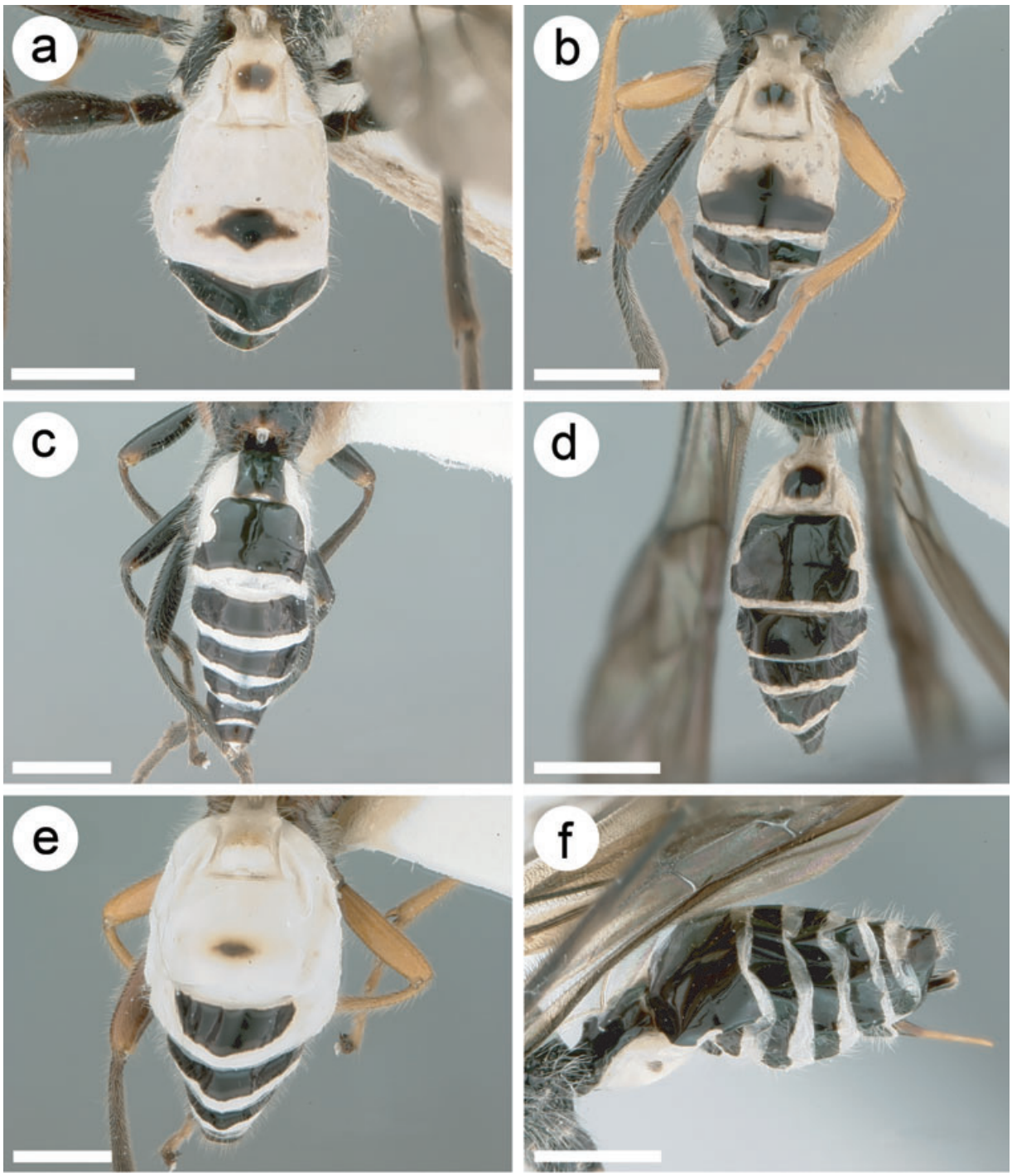

Figs 7a–f. Dorsal metasoma: a, *Maxfischeria tricolor* (holotype); b, *Maxfischeria briggsi* **sp.n.**; c, *Maxfischeria ovumancora* **sp.n.**; d, *Maxfischeria anic* **sp.n.**; e, *Maxfischeria ameliae*, **sp.n.**; f, *Maxfischeria folkertsorum*, **sp.n.**, dorsolateral view of metasoma. Scale bars: 1 mm.

Maxfischeria anic **Boring sp.n.**
(Figs 7d; 8e, f; 9a)

Diagnosis. This species can be distinguished from all other species of *Maxfischeria* by the following combination of characters: length of malar space approximately one-half the length between the tentorial pits from anterior view; propodeum almost devoid of sculpture medially, possibly with very dull anterior median carina, but otherwise smooth; length of forewing vein 1RS more than half the length of

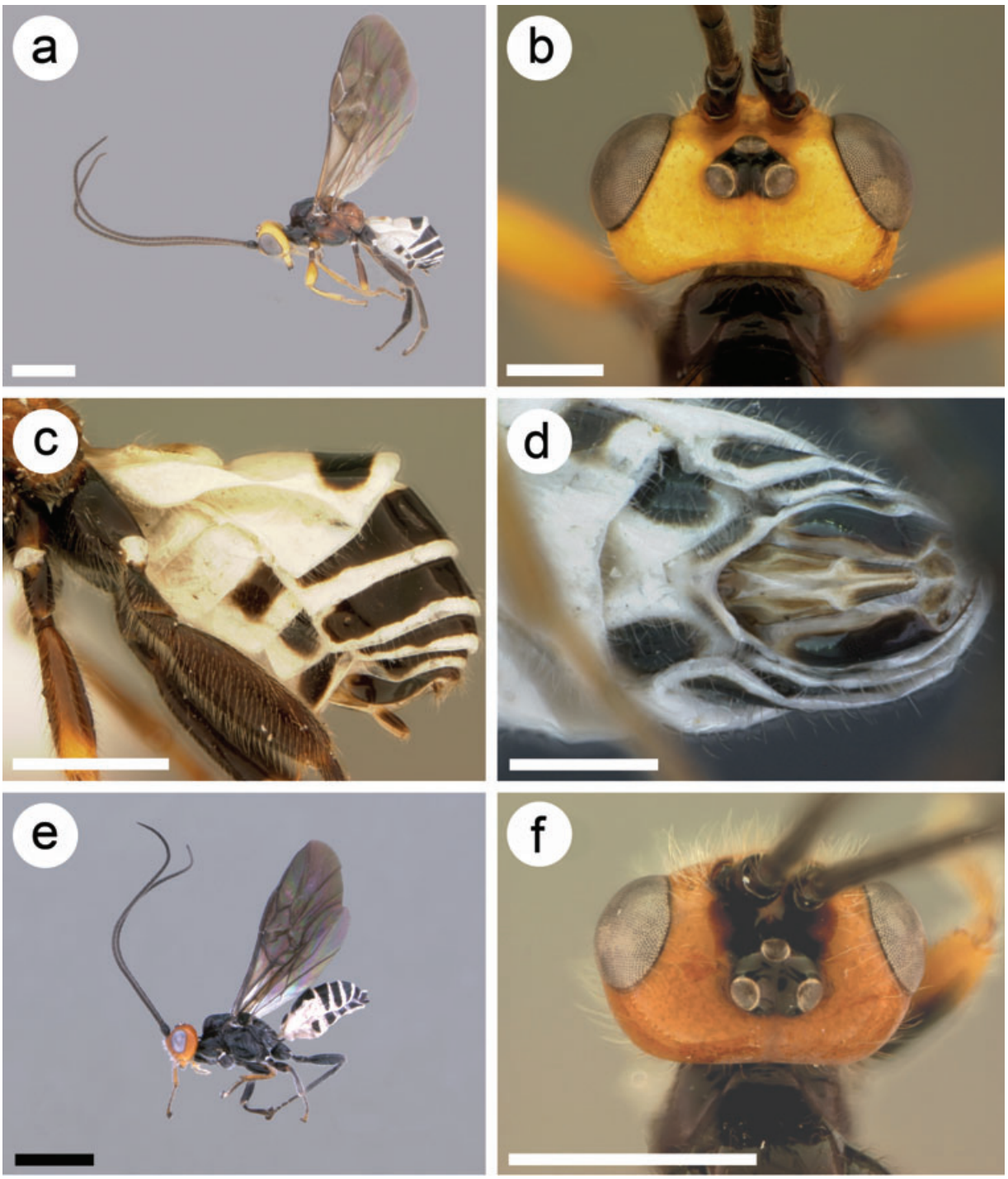

Figs 8a–f. 3–6, *Maxfischeria ameliae* **sp.n.**: a, lateral habitus, scale bar 2 mm; b, dorsal head, scale bar 0.5 mm; c, lateral metasoma, scale bar 1 mm; d, ventral metasoma, scale bar 0.5 mm; e–f, *Maxfischeria anic* **sp.n.**: e, lateral habitus, scale bar 2 mm; f, dorsal head, scale bar 0.5 mm.

forewing vein r; length of forewing vein r subequal to forewing vein 3RSa; hindwing vein 2–1A absent; metasomal median tergite 1 white with black spot (Fig. 7d); metasomal tergite 2 entirely black (Fig. 7d); hypopygium pigmented laterally (Fig. 9a).

Material examined. Holotype, 1♀, Australia, Queensland, Carnarvon Gorge National Park ranger station at light, 25°0′41″S, 148°02′03″E, 25 November 2005. N. Schiff. Deposited at ANIC, CSIRO, Canberra, ACT, Australia.

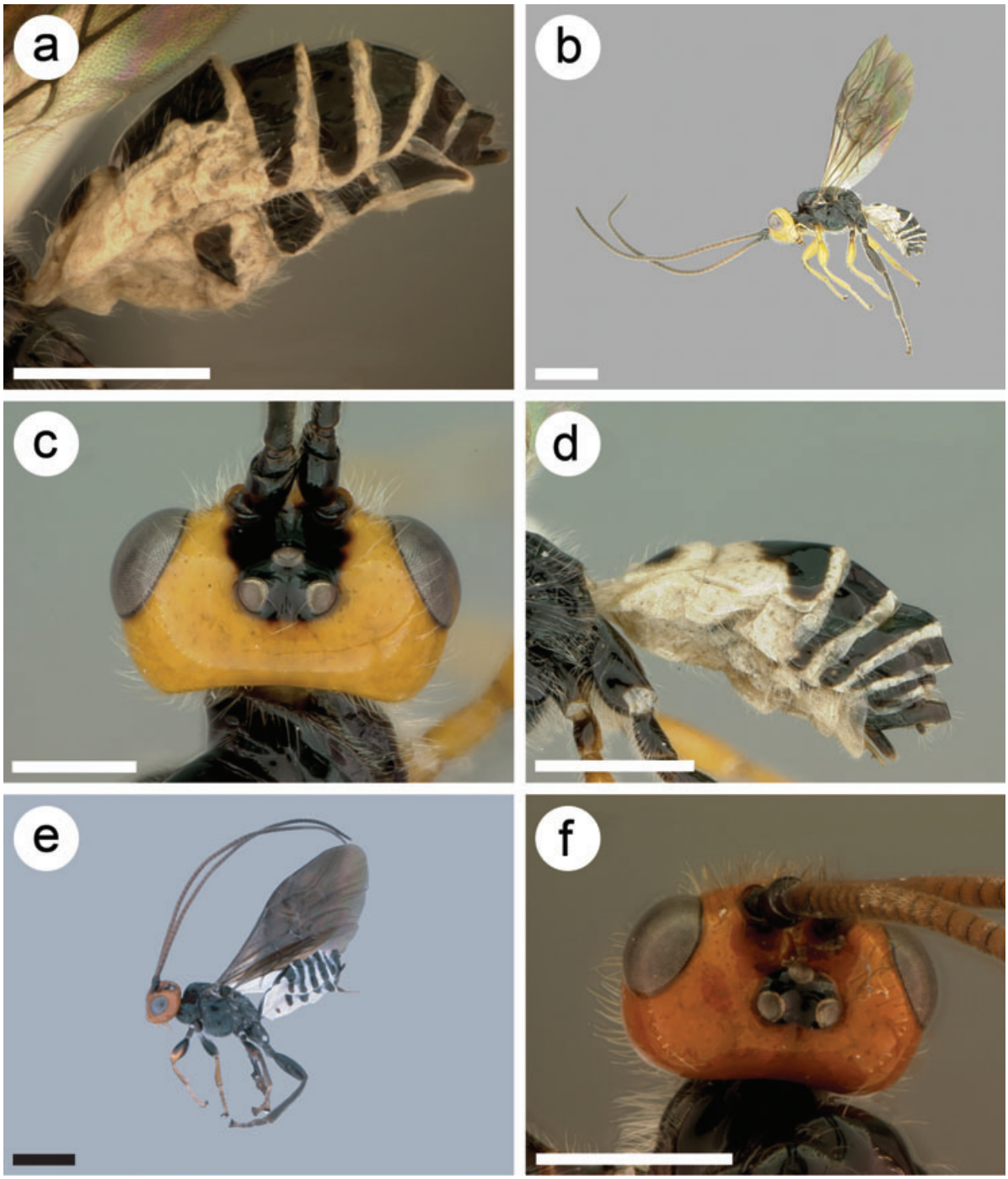

Figs 9a–f. 9, *Maxfischeria anic* **sp.n.**, lateral metasoma, scale bar 1 mm. b–d, *Maxfischeria briggsi* **sp.n.**: b, lateral habitus, scale bar 2 mm; c, dorsal head, scale bar 0.5 mm; d, lateral metasoma, scale bar 1 mm. e–f, *Maxfischeria folkertsorum*, **sp.n.**: e, lateral habitus, scale bar 2 mm; f, dorsal head, scale bar 1 mm.

Description. Length: 5.4 mm. Colour: head orange with black frons (Fig. 8f); maxillary and labial palpi yellow; scape and pedicle black, antenna flagellomeres blackish brown; base of mandible orange, reddish black at the apex; mesosoma black; fore coxa, trochanter, trochantellus, and basal portion of femur blackish brown, posterior apical portion of fore femur orange-yellow, fore tibia orange-yellow, first four tarsomeres on foreleg brown with yellow setae, apical tarsomere yellow; mid- and hindleg black basally, fading to brown apically; tegula black; wings evenly infuscate; metasomal median

tergite 1 white with black spot, median tergites 2 and 3 mostly black with white borders, median tergites 4–6 white with black bands on anterior margin, median tergites 7 and 8 entirely black (Figs 7d, 9a); metasomal sterna white except sternites 3–6 white with black bands on anterior lateral margin that do not meet ventrally (Fig. 9a); ovipositor sheath basally black and apically testaceous. Head: antenna with 41 flagellomeres, terminal flagellomere pointed, but without apical spine; ratio of malar space/tentorial length 0.52–0.56. Mesosoma: propodeum with dull anterior longitudinal median carina, propodeum otherwise smooth, setae evenly dispersed or only slightly concentrated laterally. Wings: vestigial hindwing costal vein present, vein 2–1A absent; four hamuli. Metasoma. Hypopygium medially membranous.

Distribution. This species is known from the type locality in central Queensland. Male: unknown.

Etymology. The specific epithet is a noun in apposition, named in honour of the ANIC, and all of the staff for their hard and diligent work. Additionally, the type specimen of *Maxfischeria tricolor* was borrowed from ANIC and was essential to this research.

***Maxfischeria briggsi* Boring & Sharanowski sp.n.**
(Figs 7b; 9b–d)

Diagnosis. This species can be distinguished from all other species of *Maxfischeria* by the following combination of characters: length of malar space approximately one-half the length between the tentorial pits from anterior view; propodeum sculptured, with at least an anterior median carina, areola and other irregular sculpturing; length of forewing vein 1RS more than half the length of forewing vein r; length of forewing vein r subequal to forewing vein 3RSa; hindwing vein 2–1A present but short; metasomal tergite 1 white with black spot (Fig. 7b); metasomal tergite 2 mostly white (Fig. 7b); hypopygium without pigmentation (Fig. 9d).

Material examined. Holotype, 1♀, Australia, Queensland, Carnarvon Gorge National Park ranger station at light, 25°0′41″S, 148°02′03″E, 25 November 2005. N. Schiff. Deposited at ANIC, CSIRO, Canberra, ACT, Australia.

Paratype, 1♀, Australia, Mount Kosciusko, on snow, 2133 m, 11 August 1931 L.F. Graham. Deposited at ANIC, CSIRO, Canberra, ACT, Australia.

Description. Length: 4.9–5.0 mm. Colour: head yellow with black frons (Fig. 9c); maxillary and labial palpi yellow; scape and pedicle of antenna black, flagellomeres brown; base of mandible yellow, black at apex; mesosoma black; foreleg yellow, mid leg yellow, except coxa and trochanter dark brown, hindleg black (Fig. 9b); tegula black; wings basally hyaline, apically infuscate, and with a medial hyaline streak (Fig. 9b); metasoma tergite 1 white with irregular dark-brown spot present, median tergite 2 white with irregular dark-brown mark on posterior margin, median tergites 3–7 white with black bands across anterior margin, median tergite 8 entirely black (Figs 7b, 9d); metasoma sterna white, except sternites 3 and 4 white with light brown spots laterally (Fig. 9d); ovipositor sheath dark brown; ovipositor testaceous. Head: antenna with 43 flagellomeres, terminal flagellomere with apical spine; ratio of malar space/tentorial length 0.60. Mesosoma: propodeum with dull longitudinal median carina dividing large anterior median depression, teardrop-shaped depression present just below median longitudinal carina, medial to posteromedial region with irregular small shallow depressions, large posterolateral depression bordered by carinae along posterior and lateral margin, setae concentrated laterally. Wings: hindwing costal vein absent, hindwing vein 2–1A present; four hamuli. Metasoma: hypopygium medially sclerotized.

Distribution. This species has been collected from the type locality in Queensland, Australia, and from a high elevation in New South Wales. Male: unknown.

Etymology. The specific epithet is a genitive noun, named in honour and appreciation of Reuben Briggs who was a great help in producing plates for this and other publications.

***Maxfischeria folkertsorum* Boring & Sharanowski sp.n.**
(Figs 6a, b; 7f; 9e, f)

Diagnosis. This species can be distinguished from all other species of *Maxfischeria* by the following combination of characters: length of malar space approximately one-half the length between the tentorial pits from anterior view; length of forewing vein 1RS less than half the length of forewing vein r; length of forewing vein r approximately three-quarters the length of forewing vein 3RSa; metasomal median tergite 1 entirely black (Fig. 7f).

Material examined. Holotype, 1♀, Australia, Queensland, Carnarvon Gorge National Park, ranger station at light, 25°0′41″S 148°02′03″E 25 November 2005. N. Schiff. Deposited at ANIC, CSIRO, Canberra, ACT, Australia.

Paratype, 1♀, Australia, 42.105′S, 146.08′E, 9 km WSW TAS Derwent Bridge, 21 January 1983. I.D. Naumann & J.C. Cardale.

Description. Length: 6.9 mm. Colour: head orange with black confined within ocellar triangle (Fig. 9f); maxillary and labial palpi orange–yellow; scape black, pedicel black basally, brown apically, annellus and flagellomeres light brown; mandible orange basally and reddish black apically; mesosoma black (Fig. 9e); fore coxa, trochanter, trochantellus, and basal portion of femur blackish brown, lateral apical

portion of fore femur orange–yellow, fore tibia and tarsomeres brownish yellow, mid leg dark-brown basally, fading to brownish yellow apically, hindleg dark brown; tegula black; wings evenly infuscate with a medial hyaline streak; metasoma tergite 1 entirely black, median tergites 2 and 3 mostly black with white on posterior margin of tergite 3, black band on tergite 3 extending to laterotergite 3 (Fig. 6b), median tergites 4–7 white with black bands on anterior margin, median tergite 8 entirely black (Figs 6b, 7f); metasoma sterna white, except sternite 2 white with brown spot, sternites 3–5 white with black bands on anterior lateral margin that do not meet ventrally, sternite 6 (i.e. hypopygium) white with a black band on anterior margin that meets ventrally (Fig. 6b); ovipositor sheath black basally and testaceous apically; ovipositor testaceous. Head: antenna with 56 flagellomeres, terminal flagellomere with apical spine; ratio of malar space/tentorial length 0.48–0.50. Mesosoma. Propodeum with dull anterior median longitudinal carina, with numerous irregular small deep depressions throughout, large posterolateral depression bordered by carina on posterior half, setae dispersed evenly, although absent in the posteromedian region. Wings: vestigial hindwing costal vein present, vein 2–1A absent; five hamuli on left wing, four hamuli on right wing. Metasoma: hypopygium medioposteriorly membranous in a pattern like the letter 'V'; medioanteriorly sclerotized.

Distribution. This species is known from the type locality in Queensland and from Franklin–Gordon Wild Rivers National Park in Tasmania. Male: Unknown.

Etymology. The specific epithet is a genitive noun, named in honour and appreciation of Doctors George and Debbie Folkerts for their excellence in teaching and mentoring at Auburn University.

Maxfischeria ovumancora Boring sp.n.
(Figs 17–35; 41)

Diagnosis. This species can be distinguished from all other species of *Maxfischeria* by the following combination of characters: head and propodeum melanic to dark brown (Fig. 18); length of malar space much less than one-half the length between the tentorial pits; propodeum with dull, shallow anterior longitudinal median carina (Fig. 26); hindwing vein 2–1A distinctly present and tubular; metasomal tergites 1–2 entirely black; metasoma lateral tergite 3 with a black sclerotized band (Figs 16, 19); hypopygium medially desclerotized (Fig. 20).

Material examined. Holotype, 1♀, Australia, Queensland, Carnarvon Gorge National Park ranger station at light, 25°0′41″S, 148°02′03″E, 25 November 2005. N. Schiff. Deposited at ANIC, CSIRO, Canberra, ACT, Australia.

Paratypes, 5♀, Australia, Queensland Carnarvon Gorge National Park, ranger station at light, 25°0′41″S, 148°02′03″E, 25 November 2005. N. Schiff. Deposited at ANIC, CSIRO, Canberra, ACT, Australia.

Additional specimens, 2♀, Australia, Queensland Carnarvon Gorge National Park Ranger station at light, 25°0′41″S, 148°02′03″E, 25 November 2005. N. Schiff. One specimen mounted for SEM imaging and the other dissected to examine egg morphology.

Description. Length: 5.35–6.17 mm. Colour: head blackish brown with orange spot on vertex between median ocellus and eye (Fig. 6d); maxillary and labial palpi brown, fading to testaceous; antenna brown; base of mandible orange, black at the apex; mesosoma orange, except propodeum black (Fig. 6c); fore coxa orange, fore tibia and tarsus brown with yellow tinge, mid leg and hindleg black (Fig. 6c); tegula orange; wings basally hyaline, apically infuscate, and with medial hyaline streak; metasoma tergite 1, median tergites 2 and 3 entirely black, median tergites 4–7 white with black bands on anterior margin, median tergite 8 entirely black (Figs 4e, 7c); metasomal sterna white except metasoma sternite 2 with black spot laterally, sternites 3–6 white with black bands on anterior lateral margin that do not meet ventrally (Fig. 5a); ovipositor sheath basally white and apically brown; ovipositor testaceous. Head: antenna with 42–45 flagellomeres, terminal flagellomere with apical split and spine; ratio of malar space/tentorial length 0.18–0.23. Mesosoma: propodeum with dull anterior longitudinal median carina dividing small anterior median depression, irregular shallow depressions present below median carina, posterolateral depression bordered by carinae along posterior and lateral margin, setae concentrated laterally. Wings: vestigial hindwing costal vein present, vein 2–1A present; four hamuli. Metasoma: hypopygium medially membranous (Fig. 6f).

Distribution. All known specimens are from the type locality in Queensland, Australia.

Remarks. There is no noticeable variation between the holotype and paratypes. Male: unknown.

Etymology. The specific epithet is a noun in apposition, derived from the Latin word for egg (*ovum*) and anchor (*ancora*), to reflect the anchored egg of this species.

Maxfischeria tricolor Papp, 1994
(Figs 5d–f; 7a)

Maxfischeria tricolor was described by Papp in 1994, and we agree with the original description except that the forewing vein 1cu–a (= cu–a in Papp, 1994) is subvertical, not straight; the hypostomal carina is present. The following is a redescription of the *M. tricolor* holotype. An additional seven specimens were examined to assess variation in the species.

Diagnosis. This species can be distinguished from all other species of *Maxfischeria* by the following combination of characters: length of malar space much less than one-half the length between the tentorial pits; hindwing vein 2–1A absent or occasionally an extremely small nub-like projection from 1–1A.

Material examined. Holotype, 1♀, Australia, south-east New South Wales, Kosciusko National Park, Black Derry Rest Area. 13 January 1981. at night. Leg. Hangay and Vojnits. Deposited at ANIC, CSIRO, Canberra, ACT, Australia.

Additional specimens, 7♀ (5♀) (specimens 1–4, 6), Australia, Queensland, Queensland Carnarvon Gorge National Park ranger station at light, 25°0′41″S, 148°02′03″E, 25 November 2005. N. Schiff. Specimens 2, 3 and 6 are deposited at ANIC, CSIRO, Canberra, ACT, Australia. Specimens 1 and 4 are deposited at the Hymenoptera Institute, University of Kentucky, Lexington, KY, U.S.A. (1♀) (specimen 5) Queensland, Mount Crosby, 12 November 1964, G.B. Monteith. Deposited at ANIC, CSIRO, Canberra, ACT, Australia. (1♀) (specimen 7) Canberra ACT. Dec. 1930. Deposited at ANIC, CSIRO, Canberra, ACT, Australia.

Description. Length: 6.1–7.1 mm. Colour: head yellow with black confined within ocellar triangle (Fig. 5e); maxillary and labial palpi yellow; antenna brown; base of mandible yellow, black at the apex; mesosoma black (Fig. 5d); foreleg and mid leg yellow, hindleg black; tegula black; wings evenly infuscate with medial hyaline streak; metasomal median tergite 1 white with brown spot, median tergite 2 white, median tergite 3 white with irregularly shaped black spot on anterior, median margin, median tergites 4–7 white with black bands on anterior margin, median tergite 8 entirely black (Figs 5f, 7a); metasomal sterna white, except sternites 3–6, sternite 3 white with light-brown spot on lateral margins, sternites 4 and 5 white with black bands on anterior lateral margins that do not meet ventrally, sternite 6 (= hypopygium) white with a continuous black band on anterior margin (Fig. 5f); ovipositor sheath basally white, apically brown; ovipositor testaceous. Head: 52 flagellomeres, terminal flagellomere with apical spine; ratio of malar space/tentorial length 0.27–0.30. Mesosoma: propodeum with dull anterior longitudinal median carina, propodeum otherwise smooth except for irregular small shallow depressions, setae concentrated laterally. Wings: Vestigial hindwing costal vein present, vein 2–1A absent; four hamuli. Metasoma: hypopygium sclerotized medially, membranous medioanteriorly and medioposteriorly.

Distribution. This species has been collected in Australian Capital Territory, New South Wales, and Queensland, Australia.

Remarks. Variation from the holotype is as follows. Specimen 1: head yellow with black frons; mid leg yellow except coxa and trochanter black; metasomal sterna 3–6 white with black bands on anterior lateral margin that do not meet ventrally; 46 flagellomeres; propodeum with a single elliptical-shaped depression below anterior longitudinal median carina, posterolateral depression bordered by carinae along posterior and lateral margin. Specimen 2: hindleg black, except trochanter and femur orange; metasoma T1 white with light-brown tint; metasomal sternum 6 white with black bands on anterior lateral margin that do not meet ventrally; 50 flagellomeres; propodeum with two depressions below anterior longitudinal median carina, posterolateral depression bordered by carina along posterior and lateral margin. Specimen 3: hindleg black, except trochanter and femur orange; metasoma T1 white with light-brown tint; prepectus orange; mesosoma with orange marking below sternaulus; scutellum and metanotum black with orange markings; metasoma sternites white, except sternites 5 and 6 white with black bands on anterior lateral margin that do not meet ventrally; 50 flagellomeres; propodeum with a single elliptical-shaped depression below anterior longitudinal median carina, posterolateral depression bordered by carina along posterior and lateral margin. Specimen 4: metasoma sternites 5 and 6 white with black bands on anterior lateral margin that do not meet ventrally; 47 flagellomeres; propodeum with two depressions below longitudinal anterior median carina, posterolateral depression bordered by carinae along posterior and lateral margin. Specimen 6: metasoma tergite 1 without pigmentation; three terminal metasomal sterna white with brown bands on anterior lateral margin that do not meet ventrally; antenna with 44 flagellomeres; propodeum with dull anterior longitudinal median carina. DNA was extracted from specimen 6. Male: unknown.

Acknowledgements

We thank John LaSalle and Nicole Fisher of ANIC, and Dave Briton of the Australian Museum, for hosting B. Sharanowski in May 2007 and for lending specimens. We also thank Donald Quicke (Imperial College, London, UK) for providing valuable insight on ichneumonid egg morphology. We would like to express our sincere appreciation of Nathan Schiff, for recent collection efforts in Australia, which were the source of several of the specimens examined in this paper. We extend our gratitude to the University of Kentucky Women's Club and the University of Kentucky Graduate School for crucial financial support to B. Sharanowski for travel to Australia. This research was also supported through NSF grant EF-0337220 to MJS. A final thanks to the two anonymous reviewers for their time and most helpful comments. This is paper 09-08-105 of the Agriculture Experiment Station, University of Kentucky.

References

van Achterberg, C. (1993) Illustrated key to the subfamilies of the Braconidae (Hymenoptera: Ichneumonoidea). *Zoologische Verhandelingen*, **283**, 1–189.

Belshaw, R., Dowton, M., Quicke, D.L.J. & Austin, A. (2000) Estimating ancestral geographical distributions: a gondwanan origin for

aphid parasitoids? *Proceedings of the Royal Society of London B*, **267**, 491–496.

Calendini, F. & Martin, J.-F. (2005) *PaupUP v1.0.3.1: A Free Graphical Frontend for Paup* Dos Software*. Published by the Authors, Montpellier, France [WWW document]. URL http://www.agro-montpellier.fr/sppe/Recherche/JFM/PaupUp/main.htm [accessed on 10 September 2008].

Clausen, C.P. (1932) The early stages of some tryphonine Hymenoptera parasitic on sawfly larvae. *Proceedings of the Entomological Society of Washington*, **34**, 49–60.

Coronado-Rivera, J., Gonzalez-Herrera, A., Gauld, I.D. & Hanson, P. (2004) The enigmatic biology of the ichneumonid subfamily Lycorininae. *Journal of Hymenoptera Research*, **13**, 223–227.

Edgar, R.C. (2004) MUSCLE: a multiple sequence alignment method with reduced time and space complexity. *BMC Bioinformatics*, **5**, 113.

Ellers, J. & Jervis, M.A. (2004) Why are so few parasitoid species pro-ovigenic? *Evolutionary Ecology Research*, **6**, 993–1002.

Gauld, I.D. (1976) The classification of the Anomaloninae (Hymenoptera: Ichneumonoidea). *Bulletin of the British Museum (Natural History) Entomology*, **33**, 1–135.

Goloboff, P., Farris, J. & Nixon, K. (2003) *T.N.T (Tree Analysis Using New Technology) (BETA) Version 1.0.* Published by the authors, Tucumán, Argentina.

Heraty, J. & Hawks, D. (1998) Hexamethyldisilazane: a chemical alternative for drying insects. *Entomological News*, **109**, 369–374.

Huelsenbeck, J.P. & Ronquist, F. (2001) MRBAYES: bayesian inference of phylogeny. *Bioinformatics*, **17**, 754–755.

Iwata, K. (1960) The comparative anatomy of the ovary in Hymenoptera, part V. Ichneumonidae. *Acta Hymenopterologia*, **1**, 115–169.

Jervis, M.A., Heimpel, G.E., Ferns, P.N., Harvey, J.A. & Kidd, N.A.C. (2001) Life-history strategies in parasitoid wasps: a comparative analysis of 'ovigeny'. *Journal of Animal Ecology*, **70**, 442–458.

Kartavtsev, Y. & Lee, J. (2006) Analysis of nucleotide diversity at the cytochrome b and cytochrome oxidase 1 genes at the population, species, and genus levels. *Russian Journal of Genetics*, **42**, 341–362.

Kasparyan, D.R. (1981) Ichneumonidae (Subfamily Tryphoninae) tribe Tryphonini. *Fauna of the USSR*, **106**, 1–414. [English translation of Russian original published in Leningrad].

Leys, R., Cooper, S.J.B. & Schwarz, M.P. (2000) Molecular phylogeny of the large carpenter bees, genus *Xylocopa* (Hymenoptera: Apidae), based on mitochondrial DNA sequences. *Molecular Phylogenetics and Evolution*, **17**, 407–418.

Lopez, J.V., Yuhki, N., Modi, W., Masuda, R. & O'Brien, S.J. (1994) Numt, a recent transfer and tandem amplification of mitochondrial DNA in the nuclear genome of the domestic cat. *Journal of Molecular Evolution*, **39**, 171–190.

Mason, W.R.M. (1967) Specialization in the egg structure of *Exenterus* (Hymenoptera: Ichneumonidae) in relation to distribution and abundance. *Canadian Entomologist*, **99**, 375–384.

Murphy, N., Banks, J., Whitfield, J.B. & Austin, A. (2008) Phylogeny of the parasitic microgastroid subfamilies (Hymenoptera: Braconidae) based on sequence data from seven genes, with an improved time estimate of the origin of the lineage. *Molecular Phylogenetics and Evolution*, **47**, 378–395.

Nylander, J.A.A. (2004) *MrModeltest v2. Program Distributed by the Author.* Evolutionary Biology Centre, Uppsala University, Uppsala, Sweden.

Papp, J. (1994) *Maxfischeria tricolor* gen.n. et sp.n. from Australia (Insecta: Hymenoptera: Braconidae). *Annalen des Naturhistorischen Museums Wien*, **96**, 143–147.

Posada, D. & Crandall, K.A. (1998) Modeltest: testing the model of DNA substitution. *Bioinformatics*, **14**, 817–818.

Quicke, D.L.J. (2005) Biology and immature stages of *Panteles schnetzeanus* (Hymenoptera: Ichneumonidae), a parasitoid of *Lampronia fuscatella* (Lepidoptera: Incurvariidae). *Journal of Natural History*, **39**, 431–443.

Ronquist, F. & Huelsenbeck, J.P. (2003) MRBAYES 3: bayesian phylogenetic inference under mixed models. *Bioinformatics*, **19**, 1572–1574.

Schulmeister, S., Wheeler, W.C. & Carpenter, J.M. (2002) Simultaneous analysis of the basal lineages of Hymenoptera (Insecta) using sensitivity analysis. *Cladistics*, **18**, 455–484.

Sharanowski, B.J., Dowling, A.P.G. & Sharkey, M.J. (2011) Molecular phylogenetics of Braconidae (Hymenoptera: Ichneumonoidea) based on multiple nuclear genes, and its implications for classification. *Systematic Entomology*, **36**, 549–572.

Sharkey, M.J. (1993) Family Braconidae. *Hymenoptera of the World: An Identification Guide to Families* (ed. by H. Goulet and J.T. Huber), pp. 362–395. Research Branch, Agriculture Canada and Canada Communications Group, Ottawa.

Sharkey, M.J. & Wharton, R.A. (1997) Morphology and terminology. *Manual of the New World genera of the family Braconidae* (ed. by R.A. Wharton, P.M. Marsh and M.J. Sharkey), pp. 19–38. International Society of Hymenopterists, Washington, District of Columbia.

Shaw, M.R. (2004) Notes on the biology of *Lycorina triangulifera* Holmgren (Hymenoptera: Ichneumonidae: Lycorininae). *Journal of Hymenoptera Research*, **13**, 302–308.

Smith, M.A., Wood, D.M., Janzen, D.H., Hallwachs, W. & Hebert, P.D.N. (2007) DNA barcodes affirm that 16 species of apparently generalist tropical parasitoid flies (Diptera, Tachinidae) are not all generalists. *Proceedings of the National Academy of Sciences*, **104**, 4967–4972.

Sullivan, J. & Joyce, P. (2005) Model selection in phylogenetics. *Annual Review of Ecology, Evolution, and Systematics*, **36**, 445–466.

Swofford, D.L. (2000) *PAUP*. Phylogenetic Analysis Using Parsimony (*and Other Methods). Version 4.* Sinauer Associates, Sunderland, Massachusetts.

Tajima, F. & Nei, M. (1984) Estimation of evolutionary distance between nucleotide sequences. *Molecular Biology and Evolution*, **1**, 269–285.

Tamura, K., Dudley, J., Nei, M. & Kumar, S. (2007) MEGA4: molecular evolutionary genetics analysis (MEGA) software version 4.0. *Molecular Biology and Evolution*, **24**, 1596–1599.

Townsend, A.C. & Shaw, S.R. (2009) A new species of *Andesipolis* Whitfield & Choi from the Eastern Andes of Ecuador with notes on biology and classification (Hymenoptera: Braconidae: Rhysipolinae). *Journal of Insect Science*, **9**, 1–7.

Wahl, D.B. (1993) Family Ichneumonidae. *Hymenoptera of the World: An Identification Guide to Families* (ed. by H. Goulet and J.T. Huber), pp. 395–442. Research Branch, Agriculture Canada and Canada Communications Group, Ottawa.

Zaldivar-Riverón, A., Mori, M. & Quicke, D.L.J. (2006) Systematics of the cyclostome subfamilies of braconid parasitic wasps (Hymenoptera: Ichneumonoidea): a simultaneous molecular and morphological Bayesian approach. *Molecular Phylogenetics and Evolution*, **38**, 130–145.

Zhang, D.-X. & Hewitt, G.M. (1996) Nuclear integrations: challenges for mitochondrial DNA markers. *Trends in Ecology and Evolution*, **11**, 247–251.

Accepted 5 April 2011